Published Ahead of Print on July 26, 2016 as 10.5966/sctm.2016-0006.

STEM CELLS TRANSLATIONAL MEDICINE®

TISSUE ENGINEERING AND REGENERATIVE MEDICINE

Fat-Derived Stromal Vascular Fraction Cells Enhance the Bone-Forming Capacity of Devitalized Engineered Hypertrophic Cartilage Matrix

ATANAS TODOROV,[a,b,*] MATTHIAS KREUTZ,[a,b,c,*] ALEXANDER HAUMER,[a,b] CELESTE SCOTTI,[d] ANDREA BARBERO,[a] PAUL E. BOURGINE,[a] ARNAUD SCHERBERICH,[a] CLAUDE JAQUIERY,[b,c] IVAN MARTIN[a,b]

Key Words. Bone • Bone marrow stromal cells • Adipose stromal cells • Cell transplantation • Clinical translation • Tissue regeneration

[a]Department of Biomedicine, University of Basel, Switzerland; [b]Department of Surgery and [c]Clinic for Oral and Maxillofacial Surgery, University Hospital of Basel, Basel, Switzerland; [d]Instituti di Ricovero e Cura a Carattere Scientifico, Istituto Ortopedico Galeazzi, Milano, Italy

[*]Contributed equally.

Correspondence: Ivan Martin, Ph.D., University Hospital of Basel, Hebelstrasse 20, 4031 Basel, Switzerland. Telephone: 41612652384; E-Mail: ivan.martin@usb.ch or Claude Jaquiery, M.D., D.M.D., University Hospital of Basel, Hebelstrasse 20, 4031 Basel, Switzerland. Telephone: 41612652384; E-Mail: claude.jaquiery@usb.ch

Received January 6, 2016; accepted for publication May 13, 2016.

1066-5099/2016/$20.00/0

http://dx.doi.org/10.5966/sctm.2016-0006

ABSTRACT

Engineered and devitalized hypertrophic cartilage (HC) has been proposed as bone substitute material, potentially combining the features of osteoinductivity, resistance to hypoxia, capacity to attract blood vessels, and customization potential for specific indications. However, in comparison with vital tissues, devitalized HC grafts have reduced efficiency of bone formation and longer remodeling times. We tested the hypothesis that freshly harvested stromal vascular fraction (SVF) cells from human adipose tissue—which include mesenchymal, endothelial, and osteoclastic progenitors—enhance devitalized HC remodeling into bone tissue. Human SVF cells isolated from abdominal lipoaspirates were characterized cytofluorimetrically. HC pellets, previously generated by human bone marrow-derived stromal cells and devitalized by freeze/thaw, were embedded in fibrin gel with or without different amounts of SVF cells and implanted either ectopically in nude mice or in 4-mm- diameter calvarial defects in nude rats. In the ectopic model, SVF cells added to devitalized HC directly contributed to endothelial, osteoblastic, and osteoclastic populations. After 12 weeks, the extent of graft vascularization and amount of bone formation increased in a cell-number-dependent fashion (up to, respectively, 2.0-fold and 2.9-fold using 12 million cells per milliliter of gel). Mineralized tissue volume correlated with the number of implanted, SVF-derived endothelial cells (CD31+ CD34+ CD146+). In the calvarial model, SVF activation of HC using 12 million cells per milliliter of gel induced efficient merging among implanted pellets and strongly enhanced (7.3-fold) de novo bone tissue formation within the defects. Our findings outline a bone augmentation strategy based on off-the-shelf devitalized allogeneic HC, intraoperatively activated with autologous SVF cells. STEM CELLS TRANSLATIONAL MEDICINE *2016;5:1–11*

SIGNIFICANCE

This study validates an innovative bone substitute material based on allogeneic hypertrophic cartilage that is engineered, devitalized, stored, and clinically used, together with autologous cells, intraoperatively derived from a lipoaspirate. The strategy was tested using human cells in an ectopic model and an orthotopic implantation model, in immunocompromised animals.

INTRODUCTION

Clinical treatment of challenging bone defects often requires a suitable bone graft, yet extensive donor site morbidity and complication rates around 60% [1] pose significant problems for the use of autologous bone. Commercially available bone substitute materials typically lack intrinsic osteoinductive potential, and the long-term integration into bone defects is not always achieved [2].

The use of engineered hypertrophic cartilage is receiving increasing consideration as a possible bone substitute, because of many inherent advantages. As a bradytroph and hypoxia-resistant tissue [3], it does not require immediate vascularization. Moreover, it has some initial mechanical stability, and it embeds the biological signals for remodeling into a complete bone organ, resembling the processes of embryonic bone development [4]. Although the bone-forming capacity of engineered hypertrophic cartilage has been demonstrated in stringent ectopic implantation models as well as in an orthotopic nonunion model [5–9], clinical translation can be hampered by the required use of autologous cells, their known and unpredictable variability across different donors, and the long times for in vitro construct generation.

Published Ahead of Print on July 26, 2016 as 10.5966/sctm.2016-0006.

Devitalization and off-the-shelf storage of engineered, allogeneic hypertrophic cartilage could offer an attractive bone substitute material, on the basis of the assumption that the deposited extracellular matrix (ECM) would physiologically deliver a suitable combination of cytokines and morphogens to recruit and instruct endogenous osteoprogenitors at the repair site [10]. Previous work has shown that the signals necessary for osteoinduction can be preserved in the ECM, provided a mild but effective devitalization strategy is used [11]. Yet the efficiency of bone formation remains reduced in comparison with the vital tissue. Moreover, this difference is expected to become increasingly relevant along with the graft size, because of the time required by host cells to penetrate and reactivate the matrix, a prerequisite for tissue remodeling into bone [12].

Inspired by the "developmental engineering" concept of modularity, whereby "the interfaces between developing entities are initially uncoupled" [13], here we investigated the possibility of using multiple small organoids of engineered and devitalized hypertrophic cartilage to generate a larger bone volume. The strategy is based on the rationale that each construct would efficiently develop into bone tissue as an independent module, because of the large surface-area-to-volume ratio, and the tissues would then fuse into a monolithic trabecular structure.

To enhance the reactivation and remodeling of the devitalized ECM, we further introduced the use of stromal vascular fraction (SVF) cells, freshly harvested from human adipose tissue and embedded within a gel along with the devitalized cartilage matrix. The rationale was based on the fact that SVF cells contain endothelial cells, monocytes, and mesenchymal stromal cells [14], with the respective capacity to potentially enhance tissue vascularization, osteoclast-mediated remodeling, and bone formation. Previous experiments have demonstrated that SVF cells implanted subcutaneously in a fibrin gel with hydroxyapatite granules do not form bone unless they are primed with bone morphogenetic protein (BMP)-2 [15].

The goal of the present study was thus to test the hypothesis that the supplementation of human SVF cells with multiple pellets of engineered and devitalized hypertrophic cartilage leads to a composite construct with enhanced capacity to form de novo bone tissue, both ectopically (i.e., subcutaneously in nude mice) and orthotopically (i.e., in a calvarial defect model in nude rats).

Materials and Methods

All human samples were collected with informed patient consent and after approval by the local ethical committee, in accordance with Swiss law. Animal procedures were approved by the Swiss Federal Veterinary Office (Kantonal permit BS-2590).

Preparation of Devitalized Hypertrophic Constructs

Human bone marrow stromal cells from five donors (35.4 ± 11.3 years, all male) were expanded for two passages in complete medium (α-minimum essential medium, 10% fetal bovine serum, 10 mM HEPES, 1 mM sodium pyruvate, 100 U/ml penicillin, 100 μg/ml streptomycin, 0.29 mg/ml glutamate; all from Invitrogen, Carlsbad, CA, USA, https://www.thermofisher.com) containing fibroblast growth factor-2 (5 ng/mL; R&D Systems, Minneapolis, MN, USA, https://www.rndsystems.com), as previously described [16]. Cells from different donors were used in independent experiments. Pellets were prepared by centrifuging 0.5×10^6 cells in 1.5-ml screw cap Eppendorf tubes at 300*g* for 5 minutes and cultured in serum-free medium (Dulbecco's modified Eagle's medium, 1.25 mg/ml human serum albumin, 10 mM HEPES, 1 mM sodium pyruvate, 100 U/ml penicillin, 100 μg/ml streptomycin, 0.29 mg/ml glutamate, and ITS-A [10 μg/ml insulin, 5.5 μg/ml transferrin, 5 ng/ml selenium, 0.5 mg/ml bovine serum albumin]; from Invitrogen), supplemented with 10 ng/ml transforming growth factor-β1 (R&D Systems), 10^{-7} M dexamethasone, and 0.1 mM ascorbic acid 2-phosphate (Sigma-Aldrich, St. Louis, MO, USA, https://www.sigmaaldrich.com) (chondrogenic medium). After 3 weeks, resulting cartilaginous pellets were further cultured in hypertrophic medium (serum-free medium with 50 nM thyroxine, 10 mM β-glycerophosphate, 10^{-8} M dexamethasone, 0.1 mM ascorbic acid 2-phosphate, and 50 pg/ml interleukin-1β; Sigma-Aldrich) for 2 weeks, as has been previously described [16, 17]. The generated hypertrophic pellets were devitalized by using three cycles of freezing (−196°C for 10 minutes) and thawing (37°C for 10 minutes) and a final wash with deionized water. All fluids were removed and pellets stored at −80°C until further use. To determine variability of pellets among different batches of preparation, we assessed two pellets of each donor for glycosaminoglycan (GAG) content, as has been previously described [16], and one pellet of each donor was processed histologically, as is detailed below.

Isolation of SVF Cells

SVF cells from liposuctions or excision fat were isolated from 12 donors (33.7 ± 7.7 years, 2 males and 10 females) as described previously [18, 19]. Briefly, minced fat tissue was incubated for 60 minutes in 0.15% collagenase type 2 solution, centrifuged and supernatants discarded. Cells were resuspended, filtered through 100 μm mesh filters and counted in a Neubauer counting chamber using crystal violet. Fluorescence-activated cell sorting analysis for CD31, CD34, CD146, CD90, CD105 and CD15 (AbD Serotec, Bio-Rad, Raleigh, NC, USA, https://www.bio-rad-antibodies.com) was performed, as previously described [18]. Cells were frozen in fetal bovine serum and 10% dimethyl sulfoxide and kept in the gaseous phase of liquid nitrogen until further use. Cells from different donors were used in independent experiments.

Preparation of Grafts

SVF cells were thawed and counted, and the appropriate amount was resuspended in 40 μl fibrinogen (100 mg/ml; Tisseel, Baxter, Deerfield, IL, USA, http://www.tisseel.com/). Control samples contained no SVF cells. Multiple devitalized hypertrophic pellets (12 to 24, depending on the experiment, but constant for all groups in one experiment) were mixed with this solution, and 40 μl of thrombin (400 units per milliliter with 40 μM $CaCl_2$; Baxter) were added. Polymerization was allowed to occur for 30 minutes at 37°C, followed by immediate implantation.

Ectopic and Orthotopic Implantation

For ectopic implantations, grafts were inserted into subcutaneous pouches of nude mice (CD-1 nude/nude; Charles River Laboratories, Ashland, OH, USA, http://www.criver.com/) at four pouches per mouse, with duplicate grafts per donor and experimental group. The operation was performed with isoflurane (Attane Isoflurane; Provet AG, Lyssach, Switzerland, http://www.provet.ch/) anesthesia and buprenorphine (Temgesic; Reckitt Benckiser AG,

Published Ahead of Print on July 26, 2016 as 10.5966/sctm.2016-0006.

Wallisellen, Switzerland, http://www.rb.com/) analgesia, and animals were checked periodically. After 12 weeks, mice were euthanized with CO_2, and explants were assessed, as is described below. Our previous experience with similar-sized grafts [4] suggested that 12 weeks would be sufficient for the remodeling of the cartilage pellets into bone.

For orthotopic implantations, nude rats (Rowett nude; Charles River Laboratories) were anesthetized using isoflurane, and the calvaria were exposed by dissection of the subcutaneous tissue and periosteum. Bilateral 4-mm defects were created in the central area of each parietal bone by using a saline-cooled trephine bur. The defect was refined using a piezoelectric knife in order not to injure the dura mater. The sites were constantly irrigated with sterile NaCl 0.9% to prevent overheating of the bone margins and to remove the bone debris. Grafts were molded into the defect by using a small spoon and spatula. Incisions were closed in a double layer by sutures and clamps, which were removed after 10 days. Animals were carefully monitored for behavioral abnormalities after the operation. After 4 weeks, the rats were euthanized with CO_2, followed by decapitation, and the calvaria were stored and assessed as described below.

Microtomography

After explantation, samples were fixed in 4% paraformaldehyde overnight and then transferred to phosphate-buffered saline. Microtomography was performed by using a tungsten x-ray source at 70 kV and 260 μA with an aluminum filter of 0.5 mm (Nanotome; GE, Fairfield, CT, USA, http://www.ge.com/). Transmission images were acquired for 360° with an incremental step size of 0.25°. Volumes were reconstructed using a modified Feldkamp algorithm at a voxel size of 2.5–15 μm. Manual thresholding, segmentation, and three-dimensional (3D) measurements were made with the ImageJ [20] software with the BoneJ [21] and 3DShape [22] additions.

Histology

Samples were decalcified using a 7% EDTA 30% sucrose solution (Sigma-Aldrich) and either embedded in paraffin for histological staining or frozen in optimal cutting temperature medium for immunofluorescence. Sections (5- to 10-μm thick) were stained with hematoxylin and eosin (H&E), Masson trichrome, or Safranin-O. In situ hybridization for human *Arthrobacter luteus* (ALU) sequences was performed, as has been described previously [11], to detect the presence of human cells. Tartrate resistant acid phosphatase (TRAP) staining was performed, as has been described previously [23], to identify osteoclasts. Immunohistochemistry and immunofluorescence were performed by using primary antibodies for DIPEN (1042002, MDBiosciences, St. Paul, MN, USA, http://www.mdbiosciences.com/), type X collagen (ab49945), type II collagen (ab34712), MMP13 (ab39012), MMP9 (ab38898), CD31 (ab28364), human calcitonin receptor (ab175297; all from Abcam, Cambridge, UK, http://www.abcam.com/), and human CD34 (CBL496; Dako, Glostrup, Denmark, http://www.dako.com). Secondary antibodies labeled with Alexa Fluor 488, Alexa Fluor 546, or Alexa Fluor 647 (Invitrogen) were used, and 4′,6-diamidino-2-phenylindole (DAPI) (Sigma-Aldrich) was used to stain nuclei in fluorescence images. Immunohistochemistry was done with biotinylated secondary antibodies (Dako) and the Vectastain ABC kit (Vector Laboratories, Burlingame, CA, USA, https://vectorlabs.com/). The Olympus BX61, BX63, Zeiss LSM 710, and Nikon A1R microscopes were used to acquire images.

Quantification of Histological Features

H&E-stained sections were used for the histological quantification of bone, as has been described previously [24]. Briefly, six central sections per graft, covering a total depth of 750 μm, were analyzed. The total area of the graft and the area of each pellet were manually selected, and a threshold was set to segment bone from other tissues. The bone area was then quantified as a percentage of the selected area. Osteoclasts were manually counted under high magnification on total areas of sections stained for TRAP and human calcitonin receptor, using four central sections per graft to cover a depth of 450 μm. For vessel quantification, the vessels in two representative photographs of four sections per graft, covering a total depth of 450 μm, were identified by immunofluorescence for CD31 and human CD34 and manually traced. At least four grafts per group were analyzed.

Statistical Analysis

The data were visualized and analyzed with GraphPad Prism version 6 software. Parametric analysis of variance with the appropriate post hoc tests as well as linear regressions were performed. We considered p values below .05 to indicate statistically significant differences.

Results

Devitalized Hypertrophic Constructs Activated With SVF Cells Form Ectopic Bone

Hypertrophic cartilage pellets engineered from human bone marrow-derived mesenchymal stromal cells (between 300 and 800 pellets for each of the five donors used) were rather uniform in size (average pellet diameter: 1.0 $\pm$ 0.2 mm), with variable GAG content (GAG/pellet: 15.8 $\pm$ 9.5 μg). Positive staining for GAG, type II, and type X collagen (Fig. 1A) were consistent with previously reported morphological and molecular features [16]. SVF cells from the different donors displayed a typical phenotypic heterogeneity (Fig. 1B), with the largest variability observed for the percentage of CD90 expressing cells (39.6%–86.2% of the isolated cells). After freeze/thaw devitalization, 12 pellets were suspended in a fibrin gel with or without the addition of human SVF cells (6 million cells per milliliter of gel) and implanted into nude mice (Fig. 1C).

After 12 weeks, control grafts in cell-free fibrin gel displayed depletion of glycosaminoglycans and only limited, scattered areas of remodeling into bone tissue (Fig. 2A). Instead, SVF-activated grafts contained abundant osteoid matrix, embedding large areas occupied by bone marrow. In situ hybridization for human ALU sequences indicated that the SVF-activated grafts still contained human cells surrounding the pellets after 12 weeks in vivo, in contrast to the nonactivated, devitalized grafts (Fig. 2A). However, instances of human cells surrounded by osteoid matrix were rare. A closer immunohistochemical analysis showed that both the activated and nonactivated grafts were undergoing matrix metalloproteinase (MMP)-driven degradation of cartilage matrix, leading to aggrecan cleavage, as signaled by detection of the major MMP cleavage site DIPEN (Fig. 2B). Thus, aggrecan depletion did not appear to be directly related to the efficiency of bone and bone

Published Ahead of Print on July 26, 2016 as 10.5966/sctm.2016-0006.

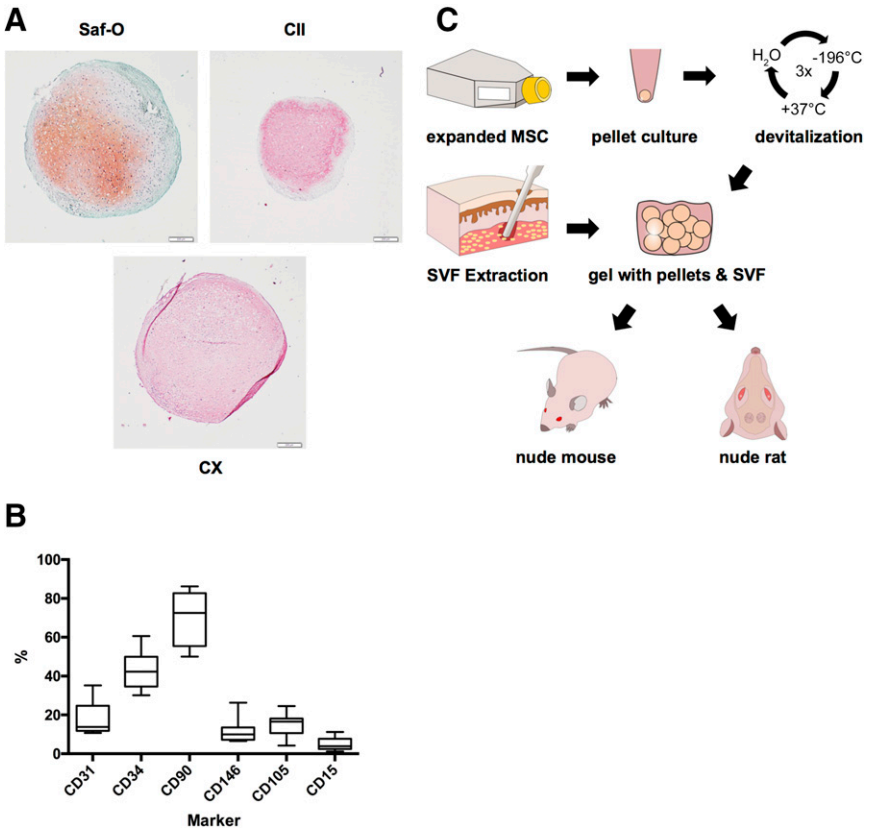

Figure 1. Starting material and experimental setup. **(A):** Representative staining of devitalized hypertrophic cartilage pellets. Scale bars = 200 μm. **(B):** Marker expression across stromal vascular fraction donors; boxes represent median with interquartile range; whiskers represent 97.5th and 2.5th percentiles. **(C):** Experimental setup for the generation of grafts, ultimately tested by implantation subcutaneously (nude mouse, ectopic model) or in calvarial defects (nude rat, orthotopic model). Abbreviations: CII, type II collagen (red/pink = positive); CX, type X collagen (red/pink = positive); MSC, mesenchymal stem cells; Saf-O, Safranin-O; SVF, stromal vascular fraction.

marrow development, which occurred to a markedly higher extent following SVF cell-based activation.

The Number of SVF Cells Correlates With Ectopic Bone Quantity

We then assessed a possible dose response in the effect of SVF cells. In up to 12 million cells per milliliter of gel, we identified a clear correlation between the number of SVF cells at implantation, and the resulting total amount of mineralized tissue, measured by microtomography (R^2 = 0.347, p = .01; Fig. 3A), or of bone matrix, quantified in histological sections (R^2 = 0.546, p = .0025; Fig. 3B). With 12 million SVF cells, the amount of bone formation was 2.9-fold higher (by histological measurements) than was the one obtained in the nonactivated grafts. It should be highlighted that quantification of the total space covered by bone structures, including bone marrow cavities embedded within the osteoid trabeculae (Fig. 3C), would lead to even more marked differences in the effect of SVF cells. The amount of bone formation was similar or even reduced by graft activation with more than 12 million SVF cells per milliliter of gel. Changes in the total amount of bone formation with the number of SVF cells were not associated with an increase in the amount of bone per pellet (Fig. 3D), but with an increase in the percentage of pellets including bone tissue (Fig. 3E). This result suggests a role of SVF cells in increasing the reproducibility of pellet remodeling.

SVF Cells Contribute to Osteoclast-Mediated Matrix Resorption

The number of implanted SVF cells correlated significantly with the density of TRAP-positive osteoclasts, histologically quantified after 12 weeks in vivo (R^2 = 0.31, p = .03; Fig. 4A, 4B). Immunofluorescence staining for the human isoform of calcitonin receptor identified some multinucleated positive cells in the vicinity of the osteoid matrix even after 12 weeks in vivo (Fig. 4C). The number of human origin osteoclasts correlated with the amount of SVF cells (R^2 = 0.32, p = .02) and represented an average of 18% of total osteoclasts when using the highest number of SVF cells (Fig. 4D). These data suggest that activation of devitalized hypertrophic cartilage by SVF cells may enhance its resorption and that SVF cells could not only attract resident osteoclasts but also offer a source for them.

Specific SVF Subpopulations of Endothelial Lineage Correlate With Total Bone Quantity

Considering the phenotypic heterogeneity of freshly isolated SVF cells, we addressed whether the amount of mineralized tissue could be correlated with the delivered dose of specific SVF subpopulations. Therefore, we analyzed data generated from graft activation by different SVF preparations (n = 9 donors) against cytofluorimetric analysis of their phenotype, performed in parallel using the markers CD31, CD34, CD146, CD90, CD105, and

Published Ahead of Print on July 26, 2016 as 10.5966/sctm.2016-0006.

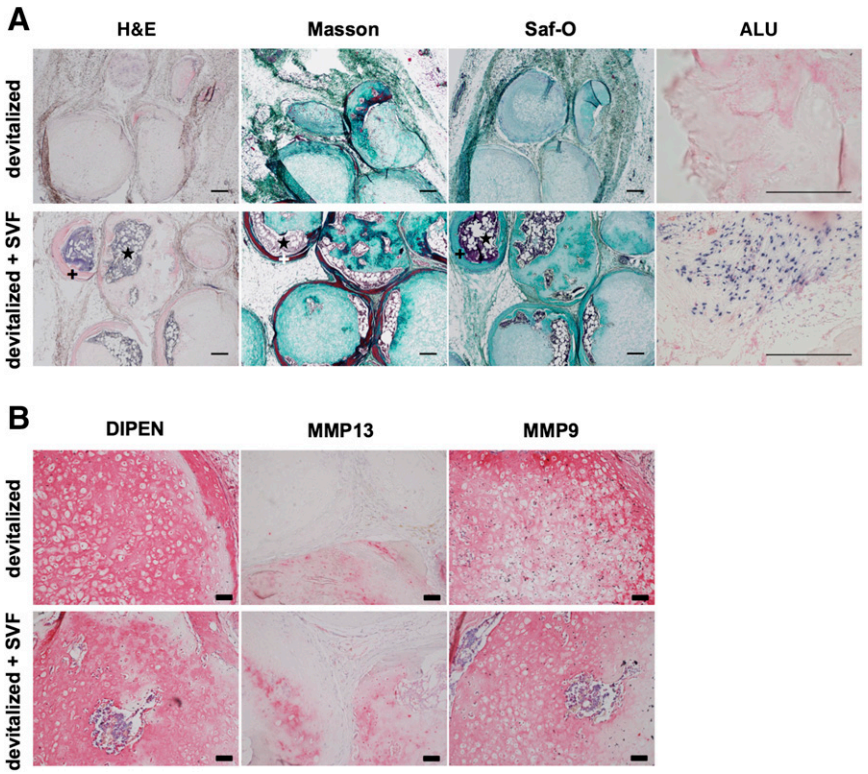

Figure 2. Ectopic bone formation. Grafts based on devitalized hypertrophic cartilage pellets were embedded in fibrin gel without or with stromal vascular fraction cells from adipose tissue and implanted subcutaneously in nude mice. **(A):** Representative hematoxylin and eosin, Masson-Tri-Chrome, and Safranin-O (Saf-O) staining and in situ hybridization for human ALU sequences (dark blue = positive) after 12 weeks in vivo. Saf-O stainings are blue-green because of lack of glycosaminoglycans and counterstaining with fast green. Osteoid matrix and bone marrow are visible. Scale bars = 200 μm. **(B):** Stainings for metalloproteinase (MMP)13 and MMP9, as well as for the N-terminal neoepitope at the major MMP cleavage site (DIPEN) after 12 weeks in vivo (red/pink = positive). Scale bars = 50 μm. +, osteoid matrix; ⋆, bone marrow. Abbreviations: ALU, *Arthrobacter luteus*; H&E, hematoxylin and eosin; Masson, Masson's trichrome; MMP, metalloproteinase; Saf-O, Safranin-O; SVF, stromal vascular fraction.

CD15. The ratio of mineralized volume to total volume correlated most strongly with the number of implanted CD31, CD34, CD146 triple-positive cells (R^2 = 0.4756, p = .013; Fig. 5A), which identify endothelial cells. No correlation was found with CD90 (R^2= 0.0226, p = .608; Fig. 5B), CD105 (R^2 = 0.0450, p = .467), or CD15 (R^2 = 0.0616, p = .392) positive cells. Staining for DAPI, type X collagen, and CD31 indicated that the activated grafts displayed a more advanced colonization of the hypertrophic matrix with uniformly organized vascular network than did the nonactivated grafts after 12 weeks in vivo (Fig. 5C, 5D). Quantification of the total length of vessels per square millimeter of section showed that grafts activated with 6 or 12 million cells per milliliter of gel were significantly more vascularized (up to 1.9-fold) than were nonactivated grafts (Fig. 5E). Immunohistochemistry for the human isoform of CD34 allowed us to identify that some of the endothelial cells lining the vessels were of human origin (Fig. 5F). The percentage of vessels including human CD34+ cells (average of 52%) and the percentage of vessel lengths formed by them (average of 29%) did not vary with the number of SVF cells seeded (Fig. 5G, 5H).

SVF-Activated Constructs Enhance Early Orthotopic Bone Formation and Bridging to Host Bone

To evaluate the orthotopic bone-regenerative capacity of SVF-activated grafts, we implanted devitalized hypertrophic cartilage pellets with or without (control) additional SVF cells (12 million per milliliter of gel) into 4 mm of rat calvarial defects (Fig. 1C). At the time of implantation the pellets were in contact with each other and with the rat calvarium. After 4 weeks, calcified volume inside the defects was nearly identical (Fig. 6A). However, more rigorous histological analysis revealed that the percentage of defect area filled by bone matrix was up to 7.3-fold larger in the SVF-activated graft than in the nonactivated grafts ($p < .0001$; Fig. 6B), with osteoid formation also reaching the center of the defect (Fig. 6C, 6D). Higher-magnification assessments indicated that bone formation in the SVF-activated group was developing by (a) remodeling of the pellets into trabecular bone organoids and (b) merging of those modular structures with each other and with the rat calvarium surrounding the defect (Fig. 6E). Both processes could not be recognized in the nonactivated grafts, also because of the minimal amounts of bone formed at the time point of observation. Pellet merging was observed in all orthotopic activated grafts, in 31% of ectopic activated grafts, and in none of the orthotopic or ectopic nonactivated grafts. In general, the size and shape of the pellets in both groups were almost identical to those of the grafts at implantation. In some areas of implants activated by SVF cells, human origin cells could be observed inside the osteoid matrix, including the areas corresponding to newly formed bone marrow sinusoids (Fig. 6F).

Published Ahead of Print on July 26, 2016 as 10.5966/sctm.2016-0006.

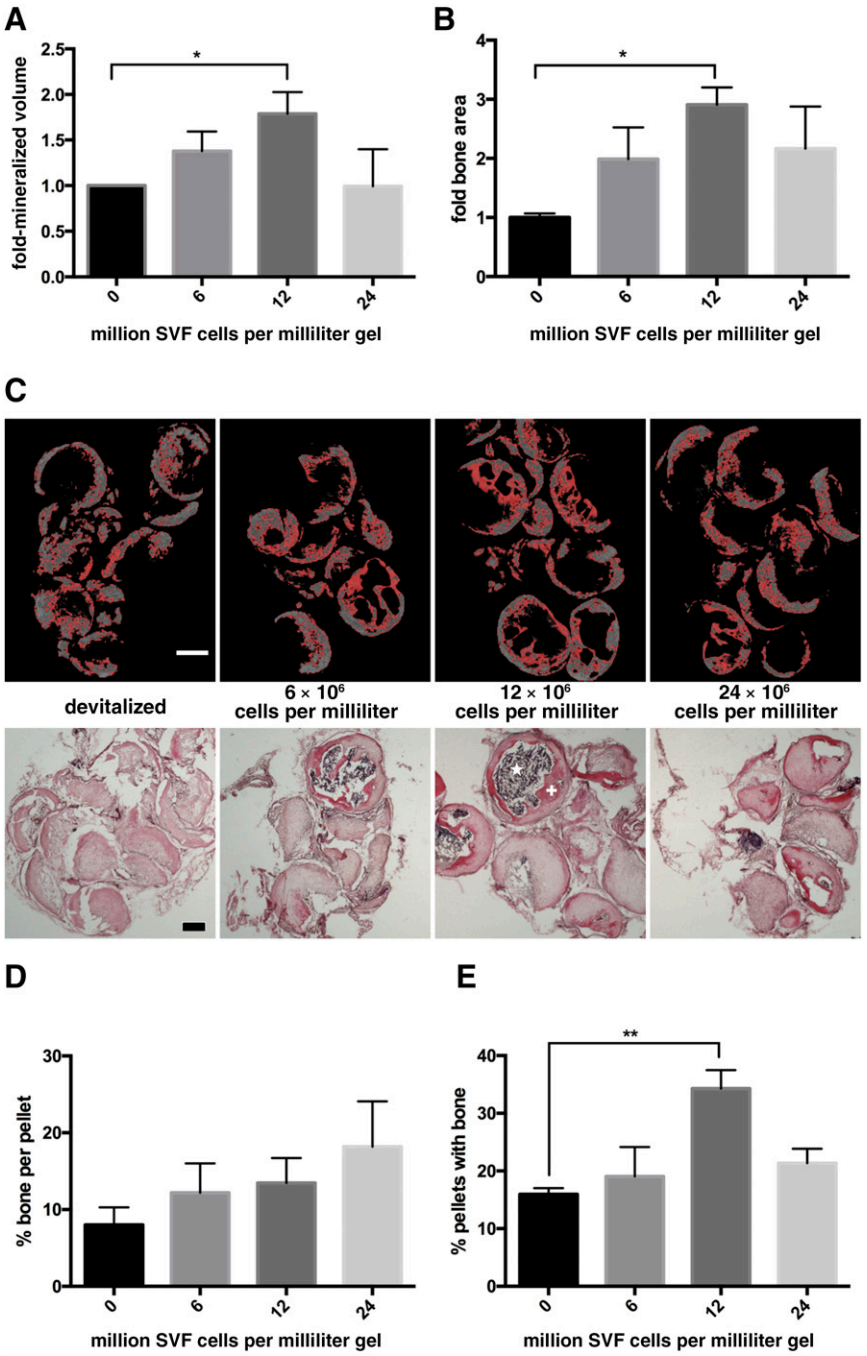

Figure 3. Effect of stromal vascular fraction (SVF) cell number. Following ectopic implantation, the amount of mineralized bone volume, quantified by microtomography **(A)** or the area covered by bone tissue, assessed in histological slides stained by hematoxylin and eosin (H&E) **(B)**, was expressed as fold difference of the nonactivated grafts and plotted versus the number of embedded SVF cells ($n = 5$–6 grafts assessed per group). $*$, $p < .05$, mean and standard error of the mean. **(C):** Representative microtomography sections, with pixels marked in red corresponding to the selected density threshold (top panels) and H&E-stained sections (bottom panels) used to generate the data displayed in panels A and B. Scale bars = 500 μm. Percentage of osteoid matrix area per total pellet area **(D)** and percentage of implanted pellets with osteoid matrix formation **(E)** ($n = 5$–6 grafts assessed per group). $**$, $p < .01$, mean and standard error of the mean. +, osteoid matrix; ⋆, bone marrow. Abbreviation: SVF, stromal vascular fraction.

Discussion

In this study we investigated the bone-forming capacity of constructs generated by the combination of devitalized engineered hypertrophic cartilage pellets with freshly isolated SVF cells from human adipose tissue. SVF activation of the hypertrophic cartilage strongly enhanced its bone-formation efficiency, tested in subcutaneous ectopic implantation and calvarial defect models. The density of SVF cells was correlated with that of osteoclasts in the grafts, and the percentage of SVF-derived endothelial lineage cells was correlated with the amount of deposited mineralized matrix.

Published Ahead of Print on July 26, 2016 as 10.5966/sctm.2016-0006.

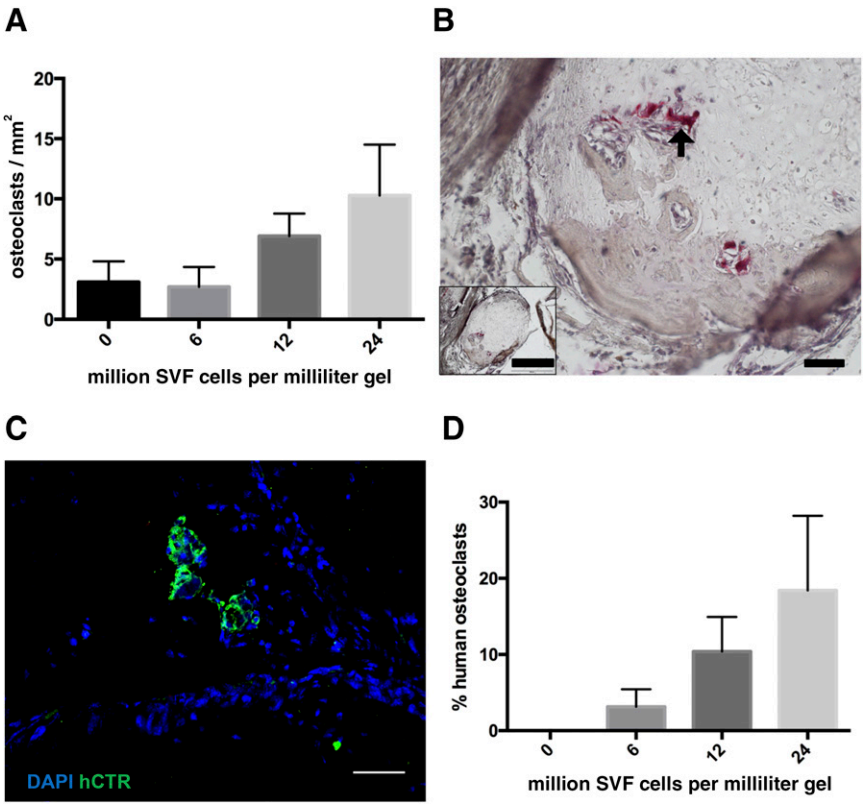

Figure 4. Osteoclast characterization. **(A):** The density of osteoclasts, assessed by tartrate resistant acid phosphatase staining (TRAP), was plotted versus the number of embedded stromal vascular fraction (SVF) cells ($n = 3$ grafts assessed per group). **(B):** Representative TRAP staining (arrow = multinucleated osteoclast). Scale bars = 50 μm or 500 μm (inset). **(C):** Staining for human calcitonin receptor (green fluorescence) indicates the direct contribution of SVF cells to osteoclast formation. Scale bar = 50 μm. **(D):** Human osteoclasts as percentage of the total number of identified osteoclasts ($n = 4$–6 grafts per group). Abbreviations: DAPI, 4′,6-diamidino-2-phenylindole; hCTR, green fluorescence; SVF, stromal vascular fraction.

The concept of using multiple pellets formed by chondrogenic differentiation of human mesenchymal stem cells (MSCs) for the engineering of bone substitute materials has been previously proposed for the treatment of segmental bone defects in immunodeficient mice [7] or rats [5]. In both studies, the cartilage grafts resulted in the generation of vascularized bone tissue, thereby supporting the idea that recapitulation of endochondral ossification is a valid strategy for bone repair at orthotopic sites. However, despite the overall good performance, limited integration across the implanted pellets was observed [7], indicating that scaling up bone graft materials by the principle of bringing together smaller modules may require further improvement. Moreover, the implantation of living tissues required the use of autologous cells, with associated cost and logistics issues.

In this context, the possibility of using engineered and then devitalized hypertrophic cartilage pellets described here would offer the distinct advantage of having "off-the-shelf" units, possibly engineered by allogeneic cells. Our results indicate that the MSC-deposited, cell-free extracellular matrix does contain the cues to trigger bone and bone marrow formation and that its effect is strongly potentiated by the activation through living progenitors derived from fat tissue. Interestingly, we observed highly efficient integration among the different pellets and with the surrounding bone areas in an orthotopic environment. The gel embedding the pellets could facilitate the ingrowing cells and the seeded SVF cells to interconnect the structures during the remodeling process. The fact that merging was more limited in an ectopic environment and absent if no SVF cells were seeded indicates that SVF cells had an effect on graft remodeling, which was enhanced by factors or cells present at a site of bone injury.

One relevant contribution of SVF cells was demonstrated to be related to the endothelial subpopulation that they include. In fact, SVF-activated grafts displayed a qualitatively more uniformly organized and quantitatively larger vascular network. Moreover, a quantitative correlation could be established between the amount of mineralized matrix formed and the density of delivered endothelial cells, phenotypically identified as expressing CD31, CD34, and CD146 [25–27]. Surprisingly, the amount of SVF cells did not correlate with the amount of human cells contributing to the vasculature after 12 weeks, despite the previously recognized role of SVF cells in establishing functional endothelial structures within engineered tissues [19, 28]. Our findings thus suggest the formation of a transitory human vasculature, followed by pruning and replacement with host vessels, or a paracrine role of the SVF-derived endothelial cells, leading to more efficient activation of resident endothelial/osteoblast lineage cell populations. Regardless of the effective mechanism, which should be addressed by analyzing early time points, our findings suggest that the number of endothelial cells in SVF preparations could be used as a quality control parameter, to ensure efficient graft activation.

Published Ahead of Print on July 26, 2016 as 10.5966/sctm.2016-0006.

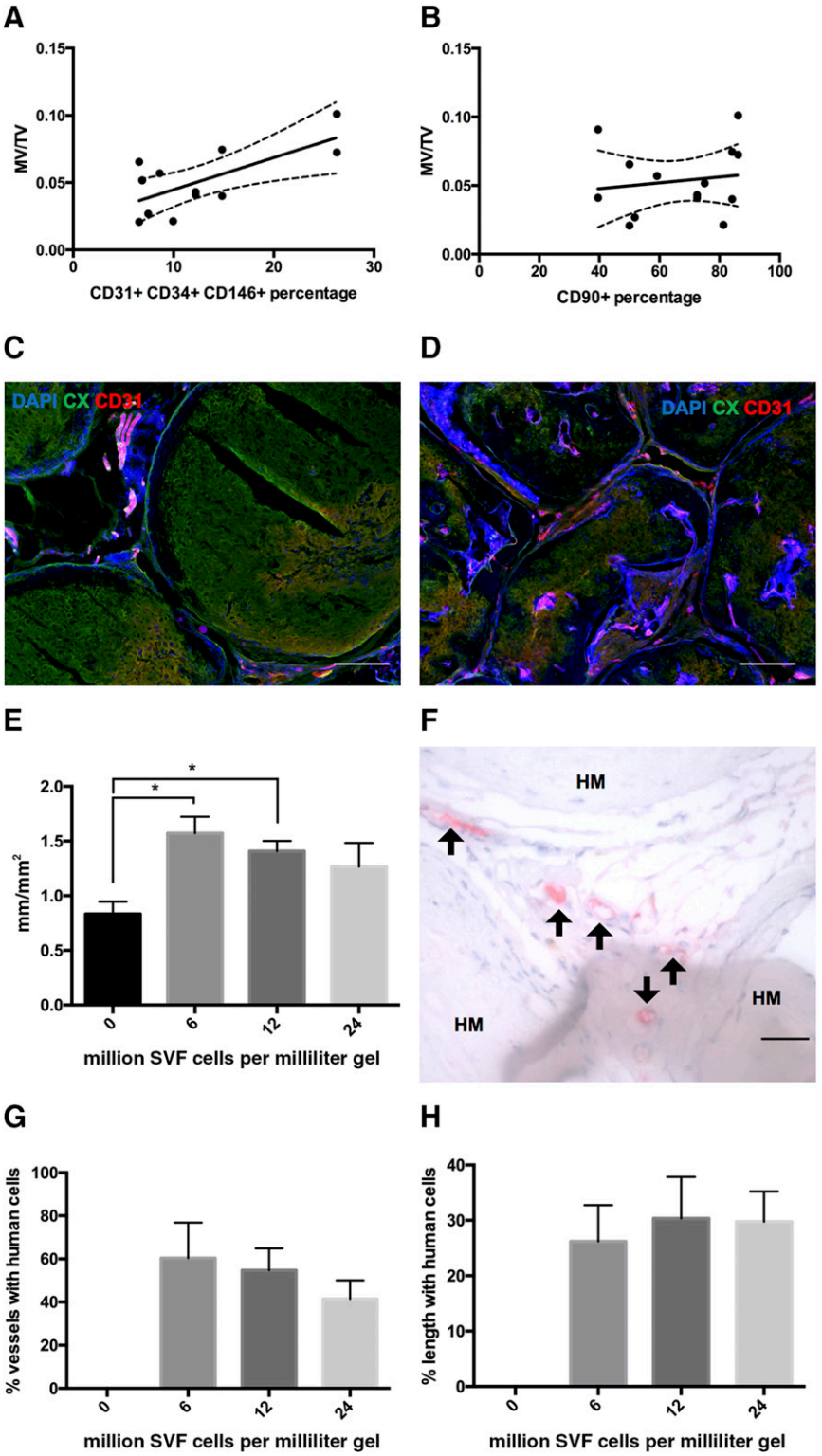

Figure 5. Contribution of stromal vascular fraction (SVF) cell lineages. Plots of mineralized tissue volume per total tissue volume versus the percentage of embedded CD31+ CD34+ CD146+ (R^2= 0.4756, p = .013) **(A)** or CD90+ SVF cells (R^2 = 0.0226, p = .608) **(B)**. Dots represent single grafts. **(C, D):** Representative immunofluorescence staining for type X collagen, CD31, and 4′,6-diamidino-2-phenylindole of devitalized samples without **(C)** or with **(D)** SVF activation after 12 weeks in vivo. Scale bars = 200 μm. **(E):** Vessel length density calculated as total length of visible vessels per square millimeter of section (n = 5–6 grafts per group). ∗, $p < .05$, mean and standard error. **(F):** Immunohistochemistry and immunofluorescence staining for human CD34, identifying positive cells (arrows) between remnants of hypertrophic matrix. Scale bars = 50 μm. Percentage of vessels with human cells **(G)** and percentage of vessel length covered by human cells (**H**) (n = 5–6 grafts per group, mean and standard error). Abbreviations: CX, type X collagen; DAPI, 4′,6-diamidino-2-phenylindole; HM, hypertrophic matrix; MV, mineralized tissue volume; SVF, stromal vascular fraction; TV, total tissue volume.

Published Ahead of Print on July 26, 2016 as 10.5966/sctm.2016-0006.

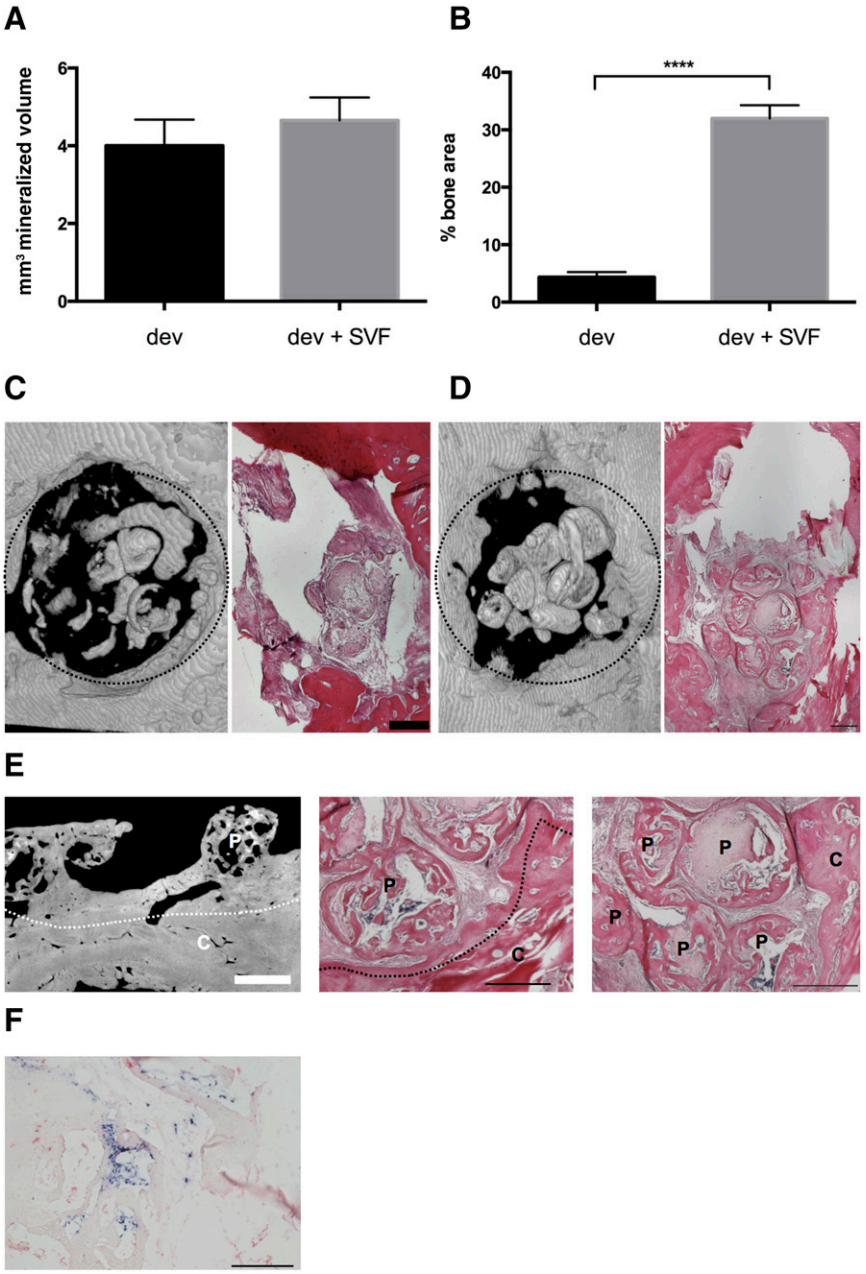

Figure 6. Bone repair capacity. Devitalized hypertrophic cartilage pellets were embedded in fibrin gel without or with stromal vascular fraction (SVF) cells from adipose tissue and implanted in rat calvarial defects. **(A):** Mineralized volume quantified by microtomography (n = 9 grafts assessed per group). **(B):** Bone area assessed in histological sections, expressed as percentage of total defect area (n = at least 24 sections assessed per group). ****, $p < .0001$. **(C, D):** Representative three-dimensional microtomography reconstructions (left) and hematoxylin/eosin (H&E) staining (right) of the calvarial defects filled with devitalized grafts, implanted without **(C)** or with **(D)** activation by SVF cells after 4 weeks. Dotted circles indicate the defect borders (4 mm diameter). Scale bars = 500 μm. **(E):** Microtomography (left) and H&E staining (middle and right) displaying the bridging between hypertrophic matrix and bone of the calvarium, or the fusion of single pellets (right) in activated grafts. White bar = 850 μm; black bars = 500 μm. Dotted lines indicate the edge of the calvarium. **(F):** In situ hybridization for *Arthrobacter luteus* sequences showing the presence of human cells (dark blue, positive) in the explants. Scale bar = 200 μm. Abbreviations: C, calvarium; dev, fibrin gel without stromal vascular fraction; dev + SVF, fibrin gel with stromal vascular fraction; P, hypertrophic matrix; SVF, stromal vascular fraction.

An increasing number of delivered SVF cells was associated with a higher density of chondroclasts/osteoclasts in the grafts. These cells were in part (5%–18% of the total) of human origin, thus derived from the monocytic population of the SVF and in part from the host, likely recruited thanks to the enhanced blood vessel invasion. A moderate increase in the density of osteoclasts from baseline values, achieved by the delivery of 12 million SVF cells per milliliter of gel, could have been pivotal at early stages in enhancing the efficiency of hypertrophic cartilage remodeling, leading to bone formation. In fact, osteoclasts would mediate release of cytokines and morphogens contained in the devitalized hypertrophic cartilage [11], in turn activating resident osteoprogenitor cells. On the other hand, a larger increase in the density of osteoclasts, corresponding to the delivery of 24 million SVF cells

Published Ahead of Print on July 26, 2016 as 10.5966/sctm.2016-0006.

per milliliter of gel, was associated with reduced bone formation. It is possible that excessive graft colonization by osteoclasts at early time points, as previously observed upon delivery of vascular endothelial growth factor [29], would disrupt bone homeostasis toward excessive degradation, ultimately resulting in more limited net amounts of bone matrix. In future studies, the timing and extent of osteoclast activity, both from the SVF donor and host, will need to be more thoroughly investigated.

Although SVF cells contain progenitors for osteoblasts, their direct contribution to the osteoid formation appeared marginal. The fact that SVF cell delivery strongly enhanced the total density of osteoblastic cells ultimately forming abundant bone matrix suggests their role in recruiting local osteoprogenitors from the host through the paracrine effect of trophic factors. An analog mode of action was recently proposed for Wharton jelly-derived mesenchymal progenitors, upon implantation in a calvarial defect [30]. Importantly, ectopic implantation of freshly harvested SVF cells in combination with calcium phosphate-based materials was previously reported to yield dense connective tissue but no bone formation [31], unless BMP-2 was additionally delivered [15]. These findings underline the strong regulatory/inductive role of the devitalized hypertrophic extracellular matrix in comparison with ceramic materials in the process of ossification. Cell populations derived from SVF culture, commonly referred to as adipose stromal cells (ASC), typically lose both endothelial and monocytic lineages and retain predominantly mesenchymal/osteoblast progenitors [19]. In light of the observed role of endothelial cells in our grafts and the almost complete absence of human osteoblasts, it will be relevant to test the hypothesis that ASC would not improve bone-forming efficiency unless a method for endothelial lineage cell preservation/expansion is used.

In our study, hypertrophic cartilage matrix was engineered, starting from bone marrow-derived MSC and subsequently devitalized. Gawlitta et al. previously proposed the use of decellularized xenogenic cartilage-derived matrix particles, also incorporated within a gel material in combination with MSC [32], and found that it induced no increase in bone tissue formation. The difference from our findings may be related to the use of articular as opposed to hypertrophic cartilage, whereby the former is phenotypically stable and developmentally not competent to support bone formation. The general approach of using engineered instead of native tissue as a source of devitalized extracellular matrix could be associated with additional advantages. In fact, an engineered matrix may be customized and enriched in defined factors (e.g., osteoinductive, angiogenic, or chemotactic cues) by using (a) specific culture medium supplements, (b) cells transduced to undergo apoptosis upon exposure to chemical agents, thereby achieving a devitalization with better preservation of the matrix [11] or (c) customized cells lines engineered to express larger amounts of the target factors [10]. Finally, it would be tempting to speculate that a devitalized extracellular matrix can be most effective in instructing formation of bone if it does not derive from the fully developed tissue but rather from the earlier stages of its development, as is the case for hypertrophic cartilage [33].

Conclusion

Our findings support a novel strategy for bone repair or augmentation, whereby allogeneic hypertrophic cartilage is engineered, devitalized, and then clinically used as an off-the-shelf material in combination with autologous SVF cells, intraoperatively derived from a lipoaspirate. Manufacturing of hypertrophic cartilage could take place within bioreactor systems, whereby biological processes could be monitored, controlled, automated, and standardized [34]. Toward clinical fruition, further studies are necessary in more relevant animal models, which should include the critical factors of immunocompetence and mechanical loading.

Acknowledgments

This work was supported by the Swiss National Science Foundation (SNF 310030_133110), the AO Foundation (AO S-11-13P), the Osteology Foundation (13-059), and the European Union (Eurostars E!7865 Endomatrix). P.E.B. is currently affiliated with the Department of Biosystems, Science, and Engineering, ETH Zurich, Basel, Switzerland.

Author Contributions

A.T. and M.K.: conception and design, collection and assembly of data, data analysis and interpretation, manuscript writing, final approval of manuscript; A.H. and P.E.B.: collection of data, data analysis and interpretation, final approval of manuscript; C.S.: conception and design, data analysis and interpretation, final approval of manuscript; A.B.: conception and design, data analysis and interpretation, manuscript writing, final approval of manuscript; A.S.: data analysis and interpretation, administrative support, provision of study material, final approval of manuscript; C.J.: data analysis and interpretation, administrative and financial support, overall supervision of animal experiments; I.M.: conception and design, data analysis and interpretation, administrative and financial support, manuscript writing, final approval of manuscript.

Disclosure of Potential Conflicts of Interest

The authors indicated no potential conflicts of interest.

References

1 Li P, Fang Q, Qi J et al. Risk factors for early and late donor-site morbidity after free fibula flap harvest. J Oral Maxillofac Surg 2015;73:1637–1640.

2 Kneser U, Schaefer DJ, Polykandriotis E et al. Tissue engineering of bone: The reconstructive surgeon's point of view. J Cell Mol Med 2006;10:7–19.

3 Grimshaw MJ, Mason RM. Bovine articular chondrocyte function in vitro depends upon oxygen tension. Osteoarthritis Cartilage 2000; 8:386–392.

4 Scotti C, Piccinini E, Takizawa H et al. Engineering of a functional bone organ through endochondral ossification. Proc Natl Acad Sci USA 2013;110:3997–4002.

5 van der Stok J, Koolen MK, Jahr H et al. Chondrogenically differentiated mesenchymal stromal cell pellets stimulate endochondral bone regeneration in critical-sized bone defects. Eur Cell Mater 2014;27:137–148; discussion 148.

6 Kuhn LT, Liu Y, Boyd NL et al. Developmental-like bone regeneration by human embryonic stem cell-derived mesenchymal cells. Tissue Eng Part A 2014;20:365–377.

7 Bahney CS, Hu DP, Taylor AJ et al. Stem cell-derived endochondral cartilage stimulates bone healing by tissue transformation. J Bone Miner Res 2014;29:1269–1282.

8 Harada N, Watanabe Y, Sato K et al. Bone regeneration in a massive rat femur defect through endochondral ossification achieved

Published Ahead of Print on July 26, 2016 as 10.5966/sctm.2016-0006.

with chondrogenically differentiated MSCs in a degradable scaffold. Biomaterials 2014;35: 7800–7810.

9 Yang W, Yang F, Wang Y et al. In vivo bone generation via the endochondral pathway on three-dimensional electrospun fibers. Acta Biomater 2013;9:4505–4512.

10 Papadimitropoulos A, Scotti C, Bourgine P et al. Engineered decellularized matrices to instruct bone regeneration processes. Bone 2015; 70:66–72.

11 Bourgine PE, Scotti C, Pigeot S et al. Osteoinductivity of engineered cartilaginous templates devitalized by inducible apoptosis. Proc Natl Acad Sci USA 2014;111:17426–17431.

12 Kojima T, Hasegawa T, de Freitas PH et al. Histochemical aspects of the vascular invasion at the erosion zone of the epiphyseal cartilage in MMP-9-deficient mice. Biomed Res 2013; 34:119–128.

13 Lenas P, Moos M, Luyten FP. Developmental engineering: a new paradigm for the design and manufacturing of cell-based products: Part I. From three-dimensional cell growth to biomimetics of in vivo development. Tissue Eng Part B Rev 2009;15:381–394.

14 Riordan NH, Ichim TE, Min WP et al. Non-expanded adipose stromal vascular fraction cell therapy for multiple sclerosis. J Transl Med 2009;7:29.

15 Mehrkens A, Saxer F, Güven S et al. Intraoperative engineering of osteogenic grafts combining freshly harvested, human adipose-derived cells and physiological doses of bone morphogenetic protein-2. Eur Cell Mater 2012; 24:308–319.

16 Scotti C, Tonnarelli B, Papadimitropoulos A et al. Recapitulation of endochondral bone formation using human adult mesenchymal stem cells as a paradigm for developmental engineering. Proc Natl Acad Sci USA 2010;107: 7251–7256.

17 Mumme M, Scotti C, Papadimitropoulos A et al. Interleukin-1β modulates endochondral ossification by human adult bone marrow stromal cells. Eur Cell Mater 2012;24:224–236.

18 Güven S, Karagianni M, Schwalbe M et al. Validation of an automated procedure to isolate human adipose tissue-derived cells by using the Sepax® technology. Tissue Eng Part C Methods 2012;18:575–582.

19 Güven S, Mehrkens A, Saxer F et al. Engineering of large osteogenic grafts with rapid engraftment capacity using mesenchymal and endothelial progenitors from human adipose tissue. Biomaterials 2011;32:5801–5809.

20 Schneider CA, Rasband WS, Eliceiri KW. NIH image to ImageJ: 25 years of image analysis. Nat Methods 2012;9:671–675.

21 Doube M, Kłosowski MM, Arganda-Carreras I et al. BoneJ: Free and extensible bone image analysis in ImageJ. Bone 2010;47:1076–1079.

22 Sheets KG, Jun B, Zhou Y et al. Microglial ramification and redistribution concomitant with the attenuation of choroidal neovascularization by neuroprotectin D1. Mol Vis 2013;19: 1747–1759.

23 Papadimitropoulos A, Scherberich A, Güven S et al. A 3D in vitro bone organ model using human progenitor cells. Eur Cell Mater 2011;21:445–458; discussion 458.

24 Martin I, Mastrogiacomo M, De Leo G et al. Fluorescence microscopy imaging of bone for automated histomorphometry. Tissue Eng 2002;8:847–852.

25 Ingram DA, Mead LE, Tanaka H et al. Identification of a novel hierarchy of endothelial progenitor cells using human peripheral and umbilical cord blood. Blood 2004;104: 2752–2760.

26 Rohde E, Bartmann C, Schallmoser K et al. Immune cells mimic the morphology of endothelial progenitor colonies in vitro. STEM CELLS 2007;25:1746–1752.

27 Yoder MC, Mead LE, Prater D et al. Redefining endothelial progenitor cells via clonal analysis and hematopoietic stem/progenitor cell principals. Blood 2007;109:1801–1809.

28 Klar AS, Güven S, Biedermann T et al. Tissue-engineered dermo-epidermal skin grafts prevascularized with adipose-derived cells. Biomaterials 2014;35:5065–5078.

29 Helmrich U, Di Maggio N, Güven S et al. Osteogenic graft vascularization and bone resorption by VEGF-expressing human mesenchymal progenitors. Biomaterials 2013;34: 5025–5035.

30 Todeschi MR, El Backly R, Capelli C et al. Transplanted umbilical cord mesenchymal stem cells modify the in vivo microenvironment enhancing angiogenesis and leading to bone regeneration. Stem Cells Dev 2015;24: 1570–1581.

31 Müller AM, Mehrkens A, Schäfer DJ et al. Towards an intraoperative engineering of osteogenic and vasculogenic grafts from the stromal vascular fraction of human adipose tissue. Eur Cell Mater 2010;19: 127–135.

32 Gawlitta D, Benders KE, Visser J et al. Decellularized cartilage-derived matrix as substrate for endochondral bone regeneration. Tissue Eng Part A 2015;21:694–703.

33 Martin I. Engineered tissues as customized organ germs. Tissue Eng Part A 2014;20: 1132–1133.

34 Martin I, Baldomero H, Bocelli-Tyndall C et al. The survey on cellular and engineered tissue therapies in Europe in 2011. Tissue Eng Part A 2014;20:842–853.

